INTL JOURNAL OF ELECTRONICS AND TELECOMMUNICATIONS, 2024, VOL. 70, NO. 4, PP. 791-796
Manuscript received September 27, 2024; revised October 2024. doi: 10.24425/ijet.2024.149610

Modeling of the characteristics of an avalanche photodiode taking into account the influence of the directed energy of the electromagnetic field

Jacek Dąbrowski, and Janusz Zarębski

***Abstract*—The paper presents and discusses the results of simulation of the current-voltage characteristics of an avalanche photodiode carried out in the SPICE program. The simulations take into account the influence of the directed energy of the electromagnetic field used in modern DEW (Directed-Energy Weapon), in the form of laser optical radiation and HPM (High Power Microwave) radiation, on the characteristics of the photodiode. The calculations were made using the model of the considered diode developed by the authors.**

***Keywords*—photodiode; DEW weapon; laser radiation; HPM radiation; modeling; SPICE**

I. Introduction

THE directed energy of the electromagnetic field is currently of great interest in the area of military technology, in particular in the development of modern DEW (Directed-Energy Weapon) [1]-[3]. The main task of such weapons using high-power energy is to destroy the enemy's technical equipment, including weapons, communication systems or autonomous reconnaissance and combat objects such as drones (UAVs - Unmanned Aerial Vehicles), as shown, among others, at work [4]. The area of potential targets also includes devices and systems that are part of critical infrastructure, e.g. ICT (Information and Communications Technology) infrastructure. High-power energy can be generated in the form of a continuous wave or HPEM (High Power Electromagnetics) pulses, in particular treated as HPM (High Power Microwave) radiation in the microwave frequency range [5]-[7] and in the form of pulsed or continuous laser radiation generated in the infrared range by high-power HEL (High Energy Lasers) [8],[9]. Intentional impact on electronic devices is called IEMI (Intentional Electromagnetic Interference) [5]. In the case of HPM, it may be indirect - the energy reaches devices through the walls of buildings and device housings, or direct - the energy penetrates devices through antennas [5],[6],[10],[11]. In turn, in the case of laser radiation, the impact is direct, because the radiation emitted by HEL or MEL (Medium Energy Laser) lasers has a thermal effect on the object it falls on, destroying it.

However, the impact of IEMI does not have to be directly destructive - in the case of directed radiation with lower powers, it temporarily disrupts the operation of electronic and optoelectronic devices and systems by changing the operating point of electronic components, including semiconductor devices [3],[9]. Ultimately, such influence may also results in the destruction of targets. Weapons using the directed energy aimed at disrupting the operation of enemy devices are called low-power (or low-energy) DEW [12],[13]. The advantage of such a weapon is its compactness and the ability to be used in a portable (mobile) form by soldiers on the battlefield. This type of weapon does not require high-power sources.

The literature review conducted by the authors does not allow to clearly determine the threshold value between low-power and high-power energy. In the case of microwave radiation, depending on the literature source, high power is treated as: a power value greater than 10 kW (average value) [14], a power value ranging from 10 to over 100 MW (pulse value) [1],[5],[15],[16]. However, in the case of optical radiation for lasers operating in the infrared, the threshold value is 1 kW [1] or 20 kW [8], but it depends on the type of laser.

Military technology that is a target for DEW weapons includes many types of optoelectronic devices and systems. These include, for example, vision systems installed on UAVs, FSO (Free Space Optics) links, thermal imaging devices, and optically guided weapons. One of the most frequently used photodetectors in optoelectronic systems are avalanche photodiodes, which, compared to pin photodiodes, are characterized by the avalanche amplification of the photocurrent, which allows for a stronger response when stimulated with a low-power optical signal [17]. Modeling of photodiodes characteristics in typical operating conditions, is presented in numerous scientific works, e.g. [18],[19]. Some of the experimental works discuss, among the others, the issue of damage of photodiodes as a result of excitation by laser radiation, e.g. [20],[21]. However, as a result of the literature review, no work was found attempting to model or present measurement studies of the impact of the directed energy on the characteristics of photodiodes with taking into account HPM and optical signals. The avalanche photodiodes, unlike pin photodiodes, typically operate with higher reverse current values. According to the authors, it may result in a higher susceptibility of these electronic elements to the impact of the directed energy of the electromagnetic field, manifested by a

All Authors are with Gdynia Maritime University, Poland (e-mail: j.dabrowski@we.umg.edu.pl, https://orcid.org/0000-0002-7504-8012, j.zarebski@we.umg.edu.pl, https://orcid.org/0000-0001-5976-1224).

change in characteristics and an operating point.

This work presents the avalanche photodiode model enabling the determination of the current-voltage characteristics of the photodiode, taking into account the influence of the directed energy of the electromagnetic field in the optical and microwave range. The SPICE program was used to develop the photodiode model, which was often used by both the authors and other researchers in the works [18],[19],[22]-[29] to develop models of various semiconductor devices, allowing for modeling their electrical and electrothermal properties. The work presents the calculation results obtained by the use of the SPICE program for selected electromagnetic field parameters and analyzes them.

II. Model Form

Figure 1 shows the network form of the worked out avalanche photodiode model. The main element of the model is the controlled G_{DIODE} current source. This source models the current flowing through the unlighted reverse biased photodiode junction (the dark current), including the recombination and diffusion currents. The photoelectric current generated in the photodiode as a result of the incident optical radiation of the useful signal is modeled by the controlled G_{OPT} current source. In turn, the photoelectric current generated as a result of disrupting optical radiation is modeled by the controlled G_{OPTD} current source.

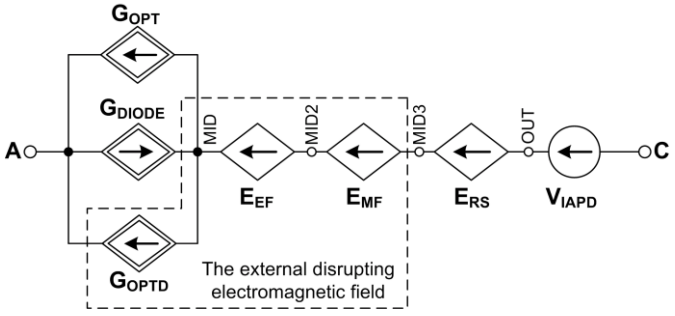

Fig. 1. The form of the avalanche photodiode model (terminals A and C represent anode and cathode of the photodiode respectively)

The controlled voltage sources E_{EF} and E_{MF} model the influence of the external electric field and the magnetic field on the characteristics of the photodiode, respectively, resulting from excitation with HPM signal. In turn, the controlled voltage source E_{RS} is responsible for modeling the voltage drop across the series resistance of the photodiode. However, the independent voltage source V_{IAPD} with a voltage efficiency of zero is an auxiliary element of the model which measure the photodiode current efficiency.

It should be noted that the influence of the electromagnetic field during HPM excitation on the characteristics of the avalanche photodiode was based on the concept presented in the co-authored work [30], in which the characteristics of the p-n diode were determined. According to this concept, the impact of the electromagnetic field on a semiconductor device can be determined by the quantities describing the variable external electric field and the variable magnetic field, i.e. the electric field intensity and the magnetic induction. As a result of the action of the electric field between the terminals of a semiconductor device, an additional voltage drop is observed, proportional to the length of the pins of such device. In turn, the alternating magnetic field induces an electromotive force between the terminals of the device, proportional to the product of the magnetic induction, the frequency of changes in the magnetic field and the dimensions of the circuit created by the terminals of the semiconductor device.

The analytical description of the G_{DIODE} source is based on the description of the p-n diode model built into the SPICE program. However, the original component of the diode current flowing in the breakdown range was removed from the considered model, and a new component related to the avalanche multiplication phenomenon was introduced to the model. This work does not present the dependencies describing the original form of the diode model from the SPICE program, given e.g. in [31],[32], but formulas modified or newly introduced into the proposed model are presented.

The current efficiency of the G_{DIODE} source in the avalanche photodiode model is described by the formula:

$$I_{GDIODE}(T,u) = \big(ID1(T,u)\cdot KINJ(T,u) + ID2(T,u)\cdot KGEN(T,u)\big)\cdot \cdot AVAL(u) \quad (1)$$

where u is the voltage between nodes A and MID, T denotes the temperature, $ID1$ is the diffusion component of the diode current, $KINJ$ is the coefficient for the high level of carrier injection, $ID2$ is the recombination current, $KGEN$ is the generation coefficient, and the $AVAL$ coefficient describes the phenomenon of the avalanche multiplication of carriers for the avalanche photodiode.

The avalanche multiplication coefficient expressed by the formula based on literature relationship presented, for example in [33],[34], is of the form:

$$AVAL(u) = \begin{cases} 1, & u \geq 0 \\ \left(1 - (u/BV_{AVAL})^{M_{AVAL}}\right), & u < 0 \end{cases} \quad (2)$$

where BV_{AVAL} is the breakdown voltage of the avalanche photodiode, and M_{AVAL} is the parameter modeling the hardness of the reverse characteristics of the avalanche photodiode. It should be noted that for the purposes of this work it was not necessary to take into account the influence of temperature on the diode breakdown voltage.

The photoelectric current generated by the useful signal modeled by the controlled current source G_{OPT} is described by the formula:

$$I_{GOPT}(u) = P_{OP}\cdot SENS\cdot AVAL(u) \quad (3)$$

where P_{OP} means the useful optical power, while the $SENS$ parameter is the maximum current sensitivity of the photodiode at the useful wavelength of optical radiation. In the case of the useful signal, it was assumed that it fell perpendicularly onto the photodiode surface.

The photoelectric current generated as a result of incident disrupting directed optical radiation, modeled by the G_{OPTD} current source, is expressed in a formula based on the theoretical relationships given in the works [19],[35],[36]:

$$I_{GOPTD}(u) = \begin{cases} (AREA\cdot q\cdot P_{OPTD}/(h\cdot c/\lambda))\cdot(1-R)\cdot \\ \cdot\big(1-exp(-\alpha\cdot W)\big)\cdot cos\theta\cdot AVAL(u), \\ c/\lambda \geq EGW/g \\ 0, \\ c/\lambda < EGW/g \end{cases} \quad (4)$$

where q is the electron charge, $AREA$ is the surface absorbing the radiation, P_{OPTD} is the optical power density of the disrupting signal, h is Planck's constant, c is the speed of light in vacuum, λ is the leading wavelength of the disrupting radiation, R is the reflection coefficient, α is the coefficient absorption of radiation, W is the width of the space charge layer of the diode junction, the parameter g is a constant corresponding to the quotient of Planck's constant by the electron charge, EGW is the width of the energy bandgap of the silicon, and Θ is the angle between the incident radiation and the normal to the photodetector surface. The radiation absorption coefficient α is described by the following relationship [35]:

$$\alpha = 5.6 \cdot 10^4 \cdot \sqrt{g \cdot c/\lambda - EGW}/(g \cdot c/\lambda) \quad (5)$$

The voltage on the controlled voltage source E_{EF}, responsible for modeling the influence of the external electric field, is expressed by the formula:

$$U_{EEF} = EF \cdot l \quad (6)$$

where EF is the external electric field intensity, and l is the physical length of the semiconductor device, including its terminals.

The voltage on the controlled voltage source E_{MF}, which is responsible for modeling the electromotive force induced in a circuit positioned perpendicular to the alternating magnetic field, is expressed as:

$$U_{EMF} = 2 \cdot \pi \cdot a \cdot b \cdot f_{MF} \cdot B_{MF} \quad (7)$$

where a and b are the dimensions of the rectangular circuit, B_{MF} is the amplitude of the magnetic induction, and f_{MF} is the frequency of changes of the magnetic field.

III. Research Results

This chapter presents the results of modeling the reverse characteristics of the avalanche photodiode using the proposed model. Calculations for the impact of individual parameters, i.e. P_{OPTD}, λ, EF, B_{MF} and f_{MF}, were performed both independently and in common at the temperature of 300 K. Moreover, values for the P_{OPTD} and EF parameters were adapted that correspond to the excitations generated by low-power DEW ($P_{OPTD} \leq$ 1 kW/m^2, $EF \leq$ 600 V/m). The photodiode model was implemented in the SPICE program in the form of a *.cir* text file.

Table I shows the parameter values of the avalanche photodiode model used in the calculations. The values putted in the white area were taken from the library of parameters of the diode model built into the SPICE program given for the photodiode MRD510 (in SPICE the parameter values are available only for this photodiode), while the parameter values given in the gray area were obtained from the following sources: catalog note for the APD50-8-150 avalanche photodiode [37] - parameters $SENS$, $AREA$ and BV_{AVAL}, the work [19] - parameter R, the work [35] - parameter W, the work [33] - parameter M_{AVAL} or adopted arbitrarily - parameters l, a, b, λ, Θ, P_{OP}. The value of the optical power of the useful signal P_{OP} falling on the photodiode was assumed on the basis of work [38], which shows that the optical powers of emitters used in FSO links are at least equaled to 10 mW. Moreover, it is worth noting that avalanche photodiode manufacturers do not provide the parameter values of the offered diodes for SPICE program.

TABLE I
PARAMETER VALUES OF THE AVALANCHE PHOTODIODE MODEL

Parameter	Value	Parameter	Value
IS [A]	$1.02 \cdot 10^{-12}$	TRS1, TRS2 [°C^{-1}], [°C^{-2}]	0
N	0.841978	SENS [A/W]	0.5
EGW [V]	1.11	BV_{AVAL} [V]	150
XTI	3	M_{AVAL}	2
RSW [Ω]	10	R	0.01
IKFW [A]	∞	AREA [m^2]	$19.6 \cdot 10^{-6}$
ISR [A]	$17 \cdot 10^{-12}$	W [m]	$1 \cdot 10^{-6}$
NR	2	l [m]	0.02
VJ [V]	0.202968	a [m]	0.01
k_M	0.146605	b [m]	0.01
FC	0.5	Θ [rad]	0.524
TIKF [°C^{-1}]	0	P_{OP} [W]	0.01
TBV1, TBV2 [°C^{-1}], [°C^{-2}]	0		

Figure 2 shows the reverse characteristics of the avalanche photodiode operating with disrupting optical radiation with a wavelength of 1100 nm for different power density values of this signal, i.e.: 0.1, 0.5, 1 kW/m^2 and in the absence of this signal. The adapted wavelength results from the proximity of the long-wave boundary of the photodiode absorption band, equalled to 1117 nm, resulting from the value of the parameter EGW. As results from the obtained calculations, the disrupting optical signal results in an increase in the photodiode current in the entire reverse bias range, but does not cause a change in the photodiode breakdown voltage. It should be noted that an additional increase in the reverse current of the photodiode may result in errors in the receiving of the correct useful optical signal or even thermal damage of a photodetector.

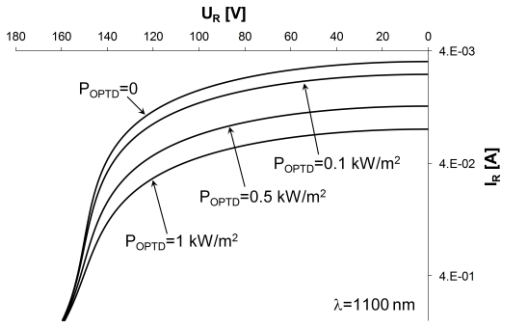

Fig. 2. Characteristics of the avalanche photodiode for different values of the power density of the optical disrupting signal

The next Fig. 3 presents the reverse characteristics of the avalanche photodiode operating in the presence of disrupting optical radiation with a constant power density of this signal equal to 1 kW/m^2 and different wavelengths of radiation, i.e. 500 nm, 1100 nm and $\lambda >$ 1117 nm. According to the obtained calculations, if the wavelength of the disrupting signal is longer than the wavelength resulting from the energy bandgap of the semiconductor material, such a signal does not affect the characteristics of the photodiode. As shown in Fig. 3, a shorter optical wave results in a smaller increase of the photoelectric current. In order to effectively and negatively affect the

photodiode, external disrupting radiation should be within the spectral sensitivity band of the photodiode.

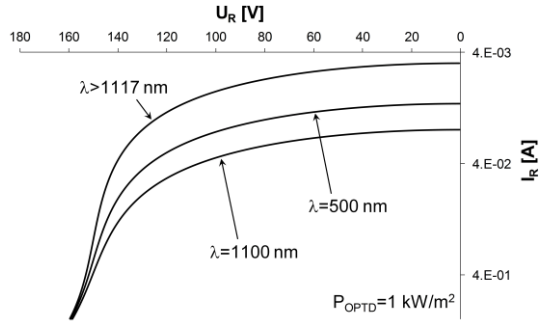

Fig. 3. Characteristics of the avalanche photodiode for different values of the wavelength of the optical disrupting signal

Figure 4 shows the reverse characteristics of the avalanche photodiode operating in the presence of a disrupting external electric field of 100 V/m, 300 V/m and 600 V/m, respectively. As it is shown by the obtained calculations, the electric field results in a decrease in the photodiode breakdown voltage and an increase in the photodiode current in the region so-called knee of the characteristics. For example, for the photodiode operating under normal conditions at the bias voltage of 140 V, after being excited by the electric field of 600 V/m, the reverse current would increase from about 40 mA to over 400 mA. Note, that such a strong increase in the photodiode current, apart from disrupting (oversaturation) the receiving path of a photoreceiver could even result in thermal damage of the photodiode.

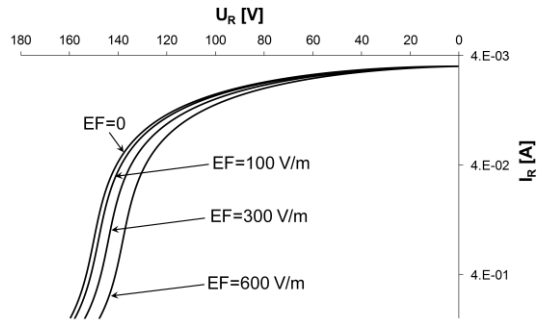

Fig. 4. Characteristics of the avalanche photodiode for different values of the intensity of the external electric field of the HPM signal

Figures 5 and 6 show the influence of the external alternating magnetic field on the reverse characteristics of the avalanche photodiode. Figure 5 presents the calculation results for a constant value of the frequency of changes in the magnetic field equal to 3 GHz and two different values of the magnetic induction: 1 μT and 2 μT. The adapted values result from the conversion of the electric field strength of 300 V/m and 600 V/m into the value of the magnetic induction. In turn, Fig. 6 presents the results obtained for the constant induction value of 1 μT and various values of the frequency of changes in the magnetic field. As can be seen from Fig. 5, the influence of the magnetic induction on the reverse characteristics of the photodiode is comparable to the influence of the electric field intensity. On the other hand, the influence of the frequency of changes in the magnetic field on the reverse characteristics of the photodiode, especially for frequency 30 GHz and 50 GHz, is clear and results in a significant increase in the reverse current and the breakdown voltage of the photodiode.

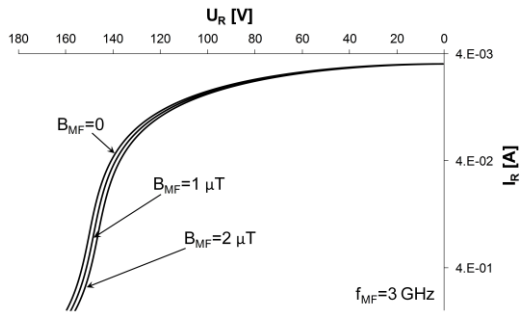

Fig. 5. Characteristics of the avalanche photodiode for different values of the magnetic induction of the HPM signal

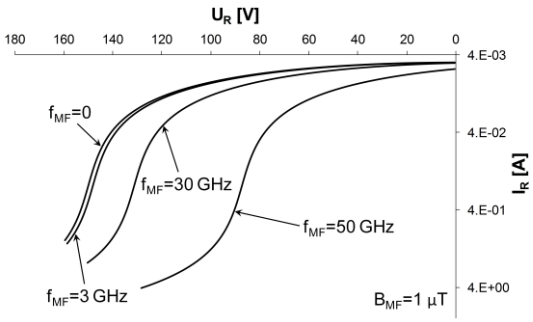

Fig. 6. Characteristics of the avalanche photodiode for different frequency values of changes in the magnetic induction of the HPM signal

Figure 7 presents the simulation results obtained for different parameter values of simultaneous optical and microwave excitation of the avalanche photodiode. The values of these parameters are given in Fig. 7. As can be seen from this figure, even weak disrupting signals, both optical and HPM, from variant no. 1 can shift the characteristic of the photodiode, disrupting the operation of this element and thus disrupting the operating of the receiving path in the photoreceiver. In the case under consideration, the wavelength of the optical signal lies outside the infrared band, i.e. in the visible band. In turn, in the second variant of excitation, the parameters of the optical signal were changed compared to the first one. An optical signal with a power density ten times higher than in the first variant and a wavelength of 1100 nm causes an increase in the reverse current from about 6 mA to about 20 mA (for small reverse voltage values respectively).

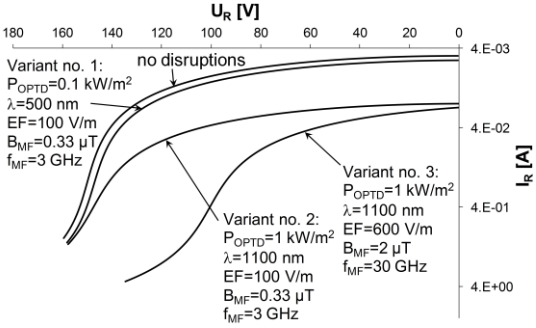

Fig. 7. Characteristics of the avalanche photodiode with the simultaneous influence of various sources of the electromagnetic field taking into account

In turn, increasing the values of parameters describing microwave disrupting excitation - variant no. 3, results in an additional increase in a reverse current and a reduction of the photodiode breakdown voltage by almost half.

IV. Summary

The paper presents a model of the silicon avalanche photodiode, dedicated to the SPICE program, proposed by the authors. The model is based partially on analytical relationships describing the isothermal model of a semiconductor diode built into the SPICE program. The model allows for the assessment of the influence of the external directed electromagnetic fields on the constant current-voltage characteristics of the avalanche photodiode under the reverse biasing. As shown by the calculations, external disrupting optical radiation results in an excessive additional reverse current, but does not reduce the breakdown voltage of the photodiode. In turn, both the external electric field and the alternating magnetic field not only cause an increase in the reverse current of the photodiode, but also significantly reduce its voltage strength by reducing the breakdown voltage. The simultaneous combination of all the disrupting factors analyzed in the work related to the directed energy of the electromagnetic field more effectively changes the shape of the photodiode's operating characteristics, which is in particular shown by the variant no. 3 of photodiode excitation in Fig. 7. The presented photodiode model requires experimental verification in the next stage of research consisting in estimating the model parameters and comparison of the obtained simulation results with the results of measurement of the characteristics of a selected commercially available avalanche photodiode excited by the directed energy of the electromagnetic field. Moreover, the model can be developed to take into account the thermal, dynamic and noise properties of the avalanche photodiode.

References

[1] Directed Energy Weapons, report GAO-23-106717, May 2023. https://www.gao.gov/assets/gao-23-106717.pdf

[2] A. De Courcy Wheeler, “Directed Energy Weapons”, Conference Paper, Convention on Certain Conventional Weapons, Geneva, 2017, pp. 1-6.

[3] D. V. Giri, R. Hoad, and F. Sabath, “Implications of High-Power Electromagnetic (HPEM) Environments on Electronics”, IEEE Electromagnetic Compatibility Magazine, Vol. 9, Q. 2, 2022, pp. 43-50, https://doi.org/10.1109/MEMC.2020.9133238.

[4] M. Z. Chaari, “High power microwave for knocking out programmable suicide drones”, Journal Security and Defence Quarterly, Vol. 34, Issue 2, 2021, pp. 68-84. https://doi.org/10.35467/sdq/135068

[5] J. Chmielińska, M. Kuchta, R. Kubacki, M. Dras, and K. Wierny, “Wybrane metody ochrony urządzeń elektronicznych przed bronią elektromagnetyczną” (Selected methods of electronic equipment protection against electromagnetic weapon), Przegląd Elektrotechniczny, R. 92, No. 1/2016, pp. 1-8, https://doi.org/10.15199/48.2016.01.01

[6] M. Dras, M. Kałuski, and M. Szafrańska, “Introduction to high power microwave as a source of disturbances”, Przegląd Elektrotechniczny, R. 92, No. 2/2016, pp. 23-25, https://doi.org/10.15199/48.2016.02.06.

[7] M. Kuchta, J. Jakubowski, and R. Kubacki, “Determinants of HPEM and HMP signal environmental measurements”, Przegląd Elektrotechniczny, R. 97, No. 12/2020, https://doi.org/10.15199/48.2020.12.45.

[8] M. Todd, “Directed Energy Technologies – Insights paper”, Emerging Disruptive Technology Assessment Symposium, November 2019. https://www.dst.defence.gov.au/sites/default/files/events/documents/Insights%20Paper%20-%20Direct%20Energy%20F1.pdf

[9] M. Spencer, “Directed Energy Weapons – Playing with Quantum Fire”, Air Power Development Centre, Australia, 2020. https://airpower.airforce.gov.au/sites/default/files/2021-03/BPAF03_Directed-Energy-Weapons.pdf

[10] M. Kuchta, J. Paś, „Broń elektromagnetyczna - zagrożenia w obiektach budowlanych” (Electromagnetic weapons - threats in building objects), Inżynieria Bezpieczeństwa Obiektów Antropogenicznych, No. 1-2, 2018, pp. 54-58.

[11] M. Budnarowska, J. Mizeraczyk, and K. Bargieł, “Development of the EM Field in a Shielding Enclosure with Aperture after Interference Caused by a Subnanosecond High-Power Parallelly Polarized EM PlaneWave Pulse”, Energies 2023, 16, 585. https://doi.org/10.3390/en16020585

[12] E. Zimet, Ch. Mann, “Directed Energy Weapons - Are We There Yet? The Future of DEW Systems and Barriers to Success”, Center for Technology and National Security Policy, National Defense University, Fort Lesley J. McNair, Washington, DC., 2009. https://www.files.ethz.ch/isn/134557/DTP%2062_Directed%20Energy%20Weapons.pdf

[13] B. Wagner, “Directed Energy: Low Power Weapons on the Rise”, National Defense, Vol. 92, No. 651, 2008, pp. 22-23.

[14] M. Suhrke, “HPEM Susceptibility of Electronic Equipment and Critical Infrastructures”, Directed Energy Systems Conference, Fraunhofer Institute for Technological Trend Analysis INT, London, 2015.

[15] D. V. Giri, F. M. Tesche, and C. E. Baum, “An Overview of High-Power Electromagnetic (HPEM) Radiating and Conducting Systems”, URSI Radio Science Bulletin, Vol. 2006, Issue: 318, pp. 6-12.

[16] A. Larsson, B. Johansson, and S. E. Nyholm, “Radiated Electric Field Strength from High-Power Microwave Systems”, 17th International Zurich Symposium on Electromagnetic Compatibility, 2006, pp. 441-444, https://doi.org/10.1109/EMCZUR.2006.214966.

[17] I. Węgrzecka, M. Węgrzecki, M. Grynglas, J. Bar, A. Uszyński, R. Grodecki, P. Grabiec, S. Krzemiński, and T. Budzyński, “Design and properties of silicon avalanche photodiodes”, Opto-Electronics Review, 12(1), 2004, pp. 95-104.

[18] F. Zappa, A. Tosi, A. Dalla Mora, and S. Tisa, “SPICE modeling of single photon avalanche diodes”, Sensors and Actuators A: Physical, 153(2009), pp. 197-204. https://doi.org/10.1016/j.sna.2009.05.007

[19] S. Z. Ahmed, S. Ganguly, Y. Yuan, J. Zheng, Y. Tan, J. C. Campbell, and A. W. Ghosh, “A Physics Based Multiscale Compact Model of p-i-n Avalanche Photodiodes”, Journal of Lightwave Technology, Vol. 39, Issue 11, 2021, pp. 3591-3598, https://doi.org/10.1109/JLT.2021.3068265.

[20] Z. Wei, G. Jin, Y. Tan, and D. Wang, “Experimental study on photodiode damage by millisecond pulse laser irradiation”, Proc. SPIE, Vol. 9671, AOPC 2015: Advances in Laser Technology and Applications. https://doi.org/10.1117/12.2197826

[21] K. Wang, X. Yu, P. Li, T. Wang, Y. Zhang, and Ch. Li, “Laser-induced damage in a silicon-based photodiode by MHz picosecond laser”, Laser Physics, Vol. 30, Issue 7, id.076002, 2020, https://doi.org/10.1088/1555-6611/ab92aa.

[22] J. Zarębski, J. Dąbrowski, “Electrothermal model of SiC power Schottky diodes”, Przegląd Elektrotechniczny, R. 87, No. 10/2011, pp. 33-38.

[23] J. Zarębski, J. Dąbrowski, “Non-isothermal Characteristics of SiC Power Schottky Diodes”, International Symposium on Power Electronics, Electrical Drives, Automation and Motion SPEEDAM, Italy, 2008, pp. 1363-1367.

[24] J. Zarębski, J. Dąbrowski, “D.C. Characteristics of SiC Power Schottky Diodes Modelling in SPICE”, Informacije MIDEM, Vol. 36, No. 3, 2006, pp. 123-126.

[25] K. Bargieł, D. Bisewski, “Evaluation of accuracy of SiC-JFET macromodel”, Computer, Applications in Electrical Engineering (ZKWE'2018), ITM Web of Conferences, Vol. 19, 01027, https://doi.org/10.1051/itmconf/20181901027.

[26] K. Górecki, J. Dąbrowski, and E. Krac, “SPICE-Aided Modeling of Daily and Seasonal Changes in Properties of the Actual Photovoltaic Installation”, Energies, 2021, 14(19), 6247. https://doi.org/10.3390/en14196247

[27] K. Górecki, J. Dąbrowski, and E. Krac, “Modeling Solar Cells Operating at Waste Light”, Energies, 2021, 14(10), 2871. https://doi.org/10.3390/en14102871

[28] J. Patrzyk, D. Bisewski, and J. Zarębski, “Electrothermal Model of SiC Power BJT”, Energies 2020, 13(10), 2617. https://doi.org/10.3390/en13102617

[29] J. Szelągowska, J. Zarębski, “Measurements and calculations of capacitances of BJT and SJT made of silicon carbide”, ITM Web of Conferences, 19:01026, January 2018, https://doi.org/10.1051/itmconf/20181901026.

[30] K. Górecki, J. Zarębski, W. J. Stepowicz, P. Górecki, D. Bisewski, K. Detka, P. Ptak, J. Dąbrowski, M. Godlewska, K. Bargieł, and J. Szelągowska, “Modelowanie wpływu zewnętrznego pola elektromagnetycznego na charakterystyki wybranych elementów elektronicznych” (Modelling an influence of an external electromagnetic field on characteristics of selected electronic components), Przegląd Elektrotechniczny, R. 95, No. 10/2019, pp.130-133, https://doi.org/10.15199/48.2019.10.29.

[31] J. Zarębski, J. Dąbrowski, “Modelling Silicon Schottky Barrier Diodes with Use of SPICE”, Computer Applications on Electrical Engineering, 2005, pp. 93-101.

[32] M. B. Wilamowski, R. C. Jaeger, “Computerized Circuit Analysis Using SPICE Programs”, McGraw-Hill Book Company, 1997.

[33] W. J. Stepowicz, “Elementy Półprzewodnikowe i Układy Scalone”, Wydawnictwo Politechniki Gdańskiej, 1999.

[34] W. Janke, “Zjawiska termiczne w elementach i układach półprzewodnikowych”, WNT, Warszawa, 1992.

[35] J. Singh, „Semiconductor Devices. Basic Principles”, John Wiley & Sons, New York, 2001.

[36] S. Fuada, A. Pratma, and T. Adiono, “Analysis of Received Power Characteristics of Commercial Photodiodes in Indoor Los Channel Visible Light Communication”, International Journal of Advanced Computer Science and Applications, Vol. 8, No. 7, 2017, pp. 164-172. http://dx.doi.org/10.14569/IJACSA.2017.080722

[37] Datasheet of APD50-8-150 avalanche photodiode: https://www.osioptoelectronics.com/media/pages/products/photodetectors/avalanche-photodiode-apd/apd10-8-150-xxxx/ce3aeedebe-1675100511/apd-series-8-150-datasheet.pdf

[38] J. Mikołajczyk, Z. Bielecki, M. Bugajski, J. Piotrowski, J. Wojtas, W. Gawron, D. Szabra, and A. Prokopiuk, “Analysis of Free-space Optics Development”, Metrology and Measurement Systems, Vol. 24 (2017), No. 4, pp. 653–674, https://doi.org/10.1515/mms-2017-0060.